

Impact of Hydrogen Surfactant Epitaxy and Annealing on Crystallinity of Epitaxial $\text{Ge}_{1-x}\text{Sn}_x$ Layers

Takanori Asano^{1,2}, Noriyuki Taoka^{1,3*}, Koya Hozaki¹, Wakana Takeuchi¹, Mitsuo Sakashita¹, Osamu Nakatsuka¹, and Shigeaki Zaima¹

¹ Graduate School of Engineering, Nagoya University, Furo-cho, Chikusa-ku, Nagoya, 464-8603, Japan

² Research Fellow of the Japan Society for the Promotion of Science, Japan

^{3*} Present affiliation: IHP, Im Technologiepark 25, 15236 Frankfurt (Oder), Germany

Phone: +81-52-789-3819, E-mail: tasano@alice.xtal.nagoya-u.ac.jp

Abstract

$\text{Ge}_{1-x}\text{Sn}_x$ growth with supplying molecular hydrogen (MH) has been examined. Molecular beam epitaxy (MBE) with MH reduces X-ray diffuse scattering and a surface roughness of $\text{Ge}_{1-x}\text{Sn}_x$ layer. Furthermore, hydrogen annealing impacts on the surface flatness. Introduction of MH into $\text{Ge}_{1-x}\text{Sn}_x$ growth promises improving on the crystallinity of $\text{Ge}_{1-x}\text{Sn}_x$.

1. Introduction

$\text{Ge}_{1-x}\text{Sn}_x$ has been a promising candidate of channel materials for metal-oxide-semiconductor field-effect transistors because electron and hole in $\text{Ge}_{1-x}\text{Sn}_x$ would have smaller effective masses than those in Ge [1]. Previously, we reported that a low temperature growth ($\sim 150^\circ\text{C}$) is a key to form a high Sn content $\text{Ge}_{1-x}\text{Sn}_x$ layer [2], although a low temperature growth would induce point defects in $\text{Ge}_{1-x}\text{Sn}_x$ layer. An annealing process after the growth is also limited due to the Sn precipitation at high temperature. These restrictions make difficult to realize both a low density of defect and a high Sn content of $\text{Ge}_{1-x}\text{Sn}_x$ epitaxial layer [3]. However, for the device applications of $\text{Ge}_{1-x}\text{Sn}_x$, we must reduce the point defect density in $\text{Ge}_{1-x}\text{Sn}_x$ because the defects seriously influence on the carrier concentration, mobility, and current conduction through defects. Therefore, an alternative technique improving the crystallinity of $\text{Ge}_{1-x}\text{Sn}_x$ must be developed. Then, we focused on the surfactant effect of hydrogen, which is known in the Ge epitaxy on Si [4]. The hydrogen surfactant suppresses the island growth and Ge segregation [4]. Furthermore, we have reported that H_2 annealing is effective at reducing the hole concentration due to defects for Ge [5]. Although the reported effects of hydrogen seem to be beneficial for $\text{Ge}_{1-x}\text{Sn}_x$, the effect for $\text{Ge}_{1-x}\text{Sn}_x$ epitaxy has not yet been elucidated. In this study, we have examined the MBE growth of $\text{Ge}_{1-x}\text{Sn}_x$ with MH, and investigated the impact of MH on the crystallinity of $\text{Ge}_{1-x}\text{Sn}_x$.

2. Experimental procedure

p-Ge(001) wafers were chemically cleaned with NH_4OH and H_2SO_4 solutions, and thermally cleaned at 430°C in a MBE chamber with a base pressure of less than 1×10^{-8} Pa. Continuously, a $\text{Ge}_{1-x}\text{Sn}_x$ layer was grown on the cleaned Ge wafer using solid-source MBE method. The film thickness and growth temperature were 100 nm and 150°C , respectively. The total pressure, P_{total} during the growth was controlled in the range between 10^{-7} and 10^{-2} Pa by varying the partial pressure of MH.

3. Results and discussion

Introduction of MH into the MBE chamber should impact on the $\text{Ge}_{1-x}\text{Sn}_x$ growth mode. The crystallinity of the $\text{Ge}_{1-x}\text{Sn}_x$ surface was observed using *in-situ* reflection high energy electron diffraction (RHEED). In the case without MH, the spotty patterns were observed (Fig. 1a). In contrast, the layer grown with supplying MH under the P_{total} of 1×10^{-2} Pa shows relatively streaky patterns (Fig. 1b). These

results indicate that the supplying MH during growth reduces the surface roughening in the atomic scale. Because the island growth of $\text{Ge}_{1-x}\text{Sn}_x$ is attributed to the misfit strain in the layer, this result indicates that the introduction of MH during the growth changes the strain in $\text{Ge}_{1-x}\text{Sn}_x$ and/or adatom diffusion on the surface.

To elucidate the effect of MH, the crystallinity of $\text{Ge}_{1-x}\text{Sn}_x$ layer was investigated using X-ray diffraction two dimensional reciprocal space mapping (XRD-2DRSM). Here, the crystallinity means the substitutional Sn content, lattice tilt, and density of point defect. Figures 2(a) and 2(b) show the results of XRD-2DRSM around the Ge $\bar{2}24$ reciprocal lattice points for the $\text{Ge}_{1-x}\text{Sn}_x$ samples grown without and with MH. From the diffraction peak positions, the substitutional Sn contents were evaluated to be 4.1% for both samples. Here, Sn content was also characterized using X-ray photoelectron spectroscopy (XPS) because we found the Sn segregation to the surface during the growth even at a low temperature of 150°C [6]. The Ge3d and Sn3d spectrums of XPS of the samples with and without MH have almost similar shapes as shown in Fig. 3. These results indicate that the Sn content at the surfaces is identical for both samples, that is, MH during the growth does not significantly affect on the Sn segregation. Furthermore, it is generally known that introduced defects cause an increase of broadening of a XRD peak. For example, a lattice tilt of epitaxial layer caused by dislocations can be observed in an increase of a full width at half maximum (FWHM) of the diffraction peak along the omega direction [7]. The phonon and defects also influence on the XRD peak shape, which is called as diffuse scattering [8]. Because the deformation of a lattice by point defects is relatively small, the scattering can be observed in the tail of Bragg diffraction [8]. In Figs. 2(a) and 2(b), the FWHMs along the omega direction of the $\text{Ge}_{1-x}\text{Sn}_x$ peaks are almost same values of 0.010° regardless of MH introduction. In Fig. 2(a), the diffuse scattering along the $[110]$ direction is observed near the Bragg diffraction of $\text{Ge}_{1-x}\text{Sn}_x\bar{2}24$ while the one in Fig. 2(b) has a weaker intensity. This difference of the diffuse scattering indicates that the point defect density in $\text{Ge}_{1-x}\text{Sn}_x$ layer is reduced by supplying MH.

The surface morphologies of these $\text{Ge}_{1-x}\text{Sn}_x$ layers were characterized using atomic force microscopy (AFM) as shown in Figs. 4(a) and 4(b). Note that there are protruding objects, which could be precipitated Sn, with the density of $7.2 \times 10^7 \text{ cm}^{-2}$ in Fig. 4(a) while no protruding objects are observed in Fig. 4(b). The RMS roughness decreases by 47% by supplying MH. Figure 5 shows the root mean square (RMS) roughness of the $\text{Ge}_{1-x}\text{Sn}_x$ layers as a function of the total pressure which was controlled by the MH partial pressure. For the samples grown with MH, a low RMS roughness was obtained because no protruding objects were observed. Hence, supplying MH is effective to obtain a flat $\text{Ge}_{1-x}\text{Sn}_x$ surface. From these results, one of the effects of supplying MH during growth is deduced to be the

reduction of the diffusion length of an adatom, resulting in a flatter surface.

To reduce the surface roughness, we have examined the annealing in N_2 and H_2 ambient. Figure 6 shows the RMS roughness of the as-grown, N_2 -, and H_2 -annealed $Ge_{0.959}Sn_{0.041}/Ge(001)$ samples, which were grown with MH, as a function of the annealing temperature. A lower RMS roughness value was obtained by a higher annealing. In particular, after hydrogen annealing at $400^\circ C$, the RMS roughness decreases to 0.23 nm. Thus, hydrogen annealing is also effective to obtain a flat surface.

Conclusions

Supplying MH with P_{total} of 1×10^{-4} Pa during $Ge_{1-x}Sn_x$ epitaxial growth reduces X-ray diffuse scattering of $Ge_{1-x}Sn_x$ and surface roughness. Hydrogen annealing after the growth is also beneficial for reducing surface

roughening. Intorrodution of MH into $Ge_{1-x}Sn_x$ epitaxy promises to improve on the crystallinity for realizing high performance $Ge_{1-x}Sn_x$ MOSFETs.

Acknowledgement

This work was partly supported by a Grant-in-Aid for Specially Promoted Research (No. 22000011) from the MEXT of Japan.

References [1] L. Low *et al.*, J. Appl. Phys. **112**, 103715 (2012). [2] Y. Shimura *et al.*, Thin Solid Films **518**, S2 (2010). [3] T. Ohmura *et al.*, JSAP Fall meeting, 18p-B4-8 (2013). [4] K. Nakagawa *et al.*, J. Crystal Growth **150**, 939 (1995). and Ohta *et al.*, Appl. Phys. Lett. **65**, 2975 (1994). [5] O. Nakatsuka *et al.*, Solid-State Electron. **83**, 82 (2013). [6] K. Kato *et al.*, Jpn. J. Appl. Phys., submitted. [7] P. Mooney *et al.*, Appl. Phys. Lett. **62**, 3464 (1993). [8] P. F. Fewster, *X-Ray Scattering from Semiconductors*, 2nd ed.: World Scientific Publishing Company (2003).

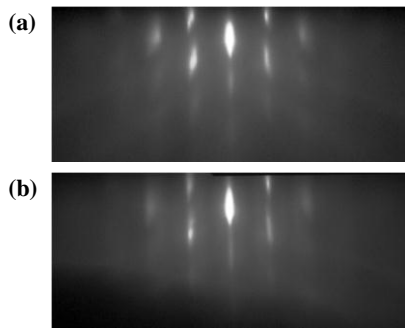


Fig. 1: RHEED patterns of $Ge_{0.959}Sn_{0.041}$ layers grown (a) without and (b) with supplying MH.

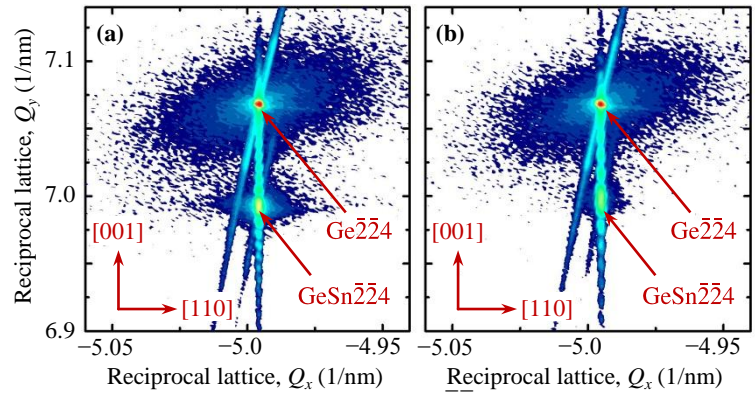


Fig. 2: XRD-2DRSM results around Ge_{224} reciprocal lattice points of $Ge_{0.959}Sn_{0.041}$ layers on Ge substrates (a) without and (b) with supplying MH.

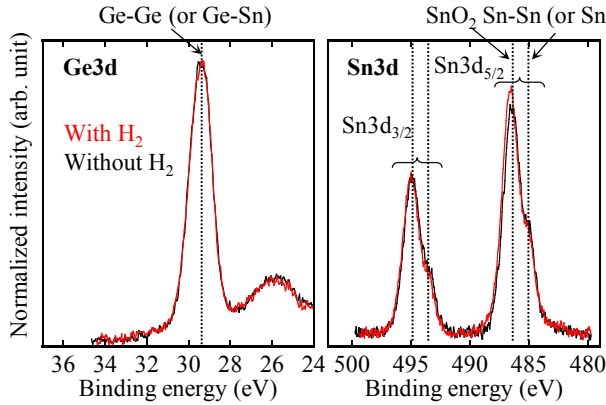


Fig. 3: Ge_{3d} and $Sn_{3d5/2}$ photoelectron core spectra of the $Ge_{1-x}Sn_x/Ge$ sample with and without MH. Intensities are normalized by the area intensity of Ge-Ge (and/or Ge-Sn) peak in Ge_{3d} spectra.

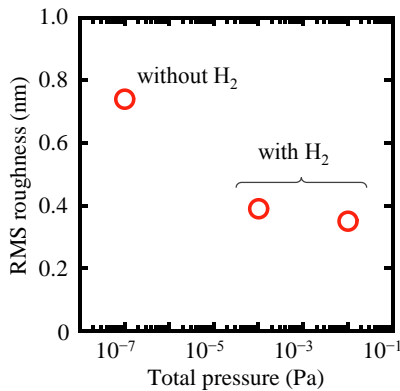


Fig. 5: RMS roughness of $Ge_{1-x}Sn_x$ layers as a function of a total pressure, which was controlled by the MH pressure.

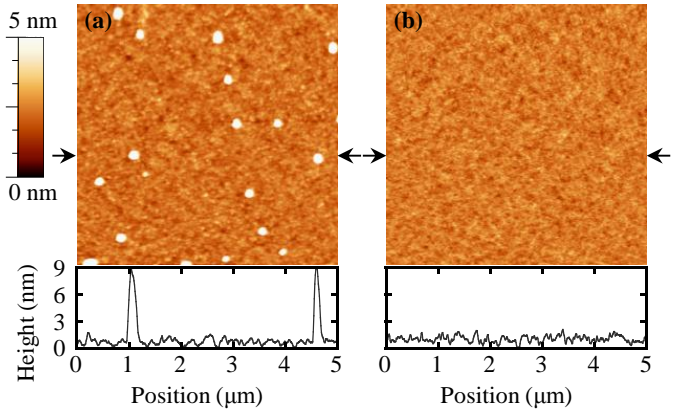


Fig. 4: AFM images and line profiles of $Ge_{1-x}Sn_x$ layers (a) without and (b) with supplying MH.

Fig. 6: RMS roughness of as-grown, N_2 -, and H_2 -annealed $Ge_{1-x}Sn_x/Ge(001)$ samples as a function of annealing temperature.

